NASA TECHNICAL NOTE

NASA TN D-2105

COMPUTATIONS FOR LARGE, UNIFORM CIRCULAR ARRAYS WITH TYPICAL ELEMENT PATTERNS

by Capers R. Cockrell

Langley Research Center
Langley Station, Hampton, Va.

NATIONAL AERONAUTICS AND SPACE ADMINISTRATION • WASHINGTON, D. C. • OCTOBER 1964

COMPUTATIONS FOR LARGE, UNIFORM CIRCULAR ARRAYS WITH TYPICAL ELEMENT PATTERNS

By Capers R. Cockrell

Langley Research Center
Langley Station, Hampton, Va.

NATIONAL AERONAUTICS AND SPACE ADMINISTRATION

For sale by the Office of Technical Services, Department of Commerce,
Washington, D.C. 20230 -- Price $0.75

COMPUTATIONS FOR LARGE, UNIFORM CIRCULAR ARRAYS WITH TYPICAL ELEMENT PATTERNS

By Capers R. Cockrell
Langley Research Center

SUMMARY

The general equation describing the total far-field pattern for circular arrays of antennas is derived in this report. By using this equation, fluctuations, obtained by varying the azimuthal angle through 360°, were calculated and plotted as a function of circumference in wavelengths for three typical element patterns. A wide range of circumferences was chosen so that the graphs include frequencies which permit practical circular arrays for space vehicles. The circumference in wavelengths ranges from 1 to 60 while the number of antennas range from 3 to 70.

INTRODUCTION

An interesting as well as useful antenna configuration is that of circular arrayed antennas. Since the shapes of many space vehicles are circularly symmetrical, the arraying of antennas in a circle is suitable and logical. This arrangement of antennas gives a symmetrical pattern in the far field as the vehicle rolls in space.

The equation which describes the far-field radiation pattern for circular arrays is derived in detail in this report. For the particular arraying being discussed, the resulting expression is of Bessel form. In this Bessel expression the argument is dependent upon the frequency and phase center of the array.

Although the general equation is valid for an infinite number of element patterns, this report is concerned primarily with only three elements, as shown in sketch (a). These typical element patterns were chosen because they are representative of the types used in circular arrays.

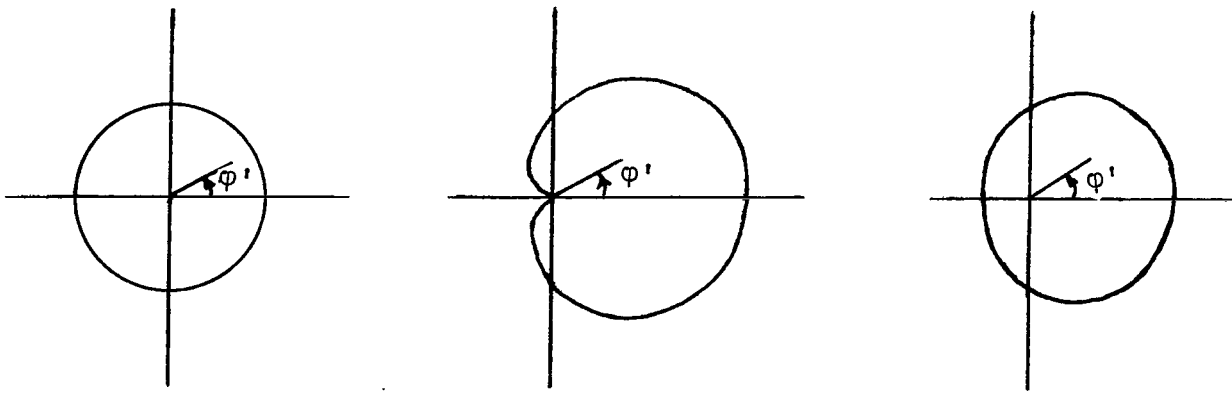

$F(\varphi') = 1$ $\qquad$ $F(\varphi') = 1 + \cos\varphi'$ $\qquad$ $F(\varphi') = 1 + \frac{1}{2}\cos\varphi'$

Sketch (a)

The primary objective of this report is to give a set of graphs which are useful in determining the fluctuation in the far-field pattern for circular arrayed antennas. The fluctuation, defined as $20 \log_{10} \frac{|\Phi|_{max}}{|\Phi|_{min}}$, is plotted as a function of circumference in wavelengths Z. The ratio $\frac{|\Phi|_{max}}{|\Phi|_{min}}$ is determined by the maximum and minimum magnitudes which are measured in the far field. A wide range of circumferences was chosen so that the graphs include frequencies which permit practical circular arrays for space vehicles. The circumference in wavelengths ranges from 1 to 60 while the number of sources S or antennas range from 3 to 70.

SYMBOLS

a	radius of array
$a_r = \frac{2\pi a}{\lambda}$	
A_n, a_n	coefficients of Fourier cosine series
i	represents i-source, 1, 2, 3, . . . S
$J_S(Z)$	ordinary Bessel function of first kind
j	imaginary number, $\sqrt{-1}$
k	wave number, $2\pi/\lambda$
n	integer

N	upper limit of the Fourier cosine series
q	integer, m/S
S	number of antennas (sources)
u_i	angular spacing between antennas, $2\pi i/S$, radians
x,y	rectangular coordinates
Z	circumference in wavelengths
$F(\varphi')$	element pattern
δ_{om}	Kronecker delta $(\delta_{om} = 1 \text{ for } m = 0 \text{ and } \delta_{om} = 0 \text{ for } m \neq 0)$
λ	wavelength
ψ_i	distance in radians between center of array and i-antenna in direction of far-field point
Φ	far-field pattern
φ	angle of far-field point, radians
φ'	modified angle of far-field point, radians

Subscripts:

max	maximum
min	minimum

DERIVATION OF BASIC EQUATION

The derivation of the total far-field pattern for a linear array of antennas which are identical, equally spaced, and fed in phase is one of simple geometry; therefore, no major difficulties are encountered. (See ref. 1.) For the linear array, a single array factor can be determined; but in a circular array, a single array factor is not obtainable. Because of the circular arrangement there is a phase difference which changes as the number of antennas vary. In the case of a circular array, the general equation of the total far-field pattern has a solution that is of Bessel form. This equation was originally derived by Chu. (See ref. 2.) The calculations given by Chu have been extended to cover values of circumferences and number of sources considerably larger than presently available.

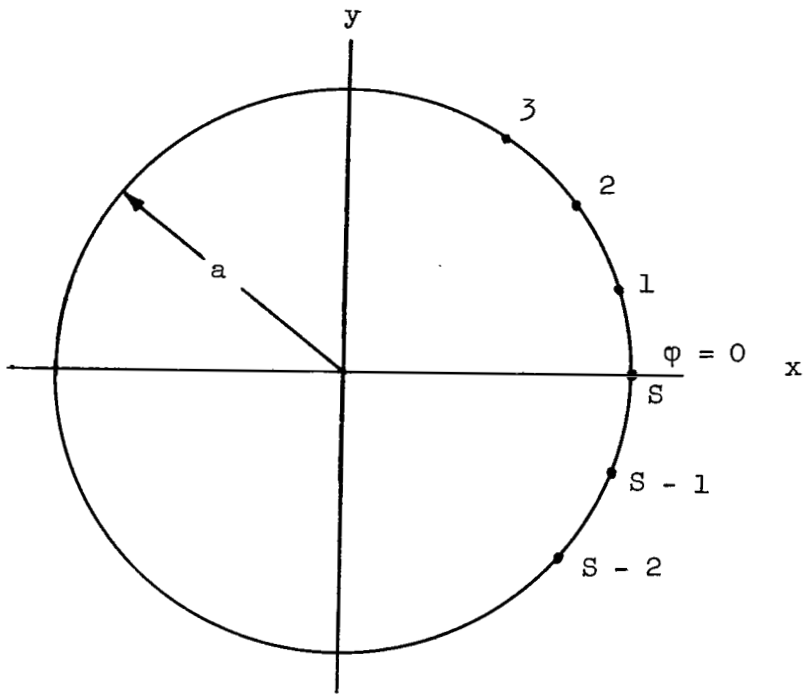

Sketch (b)

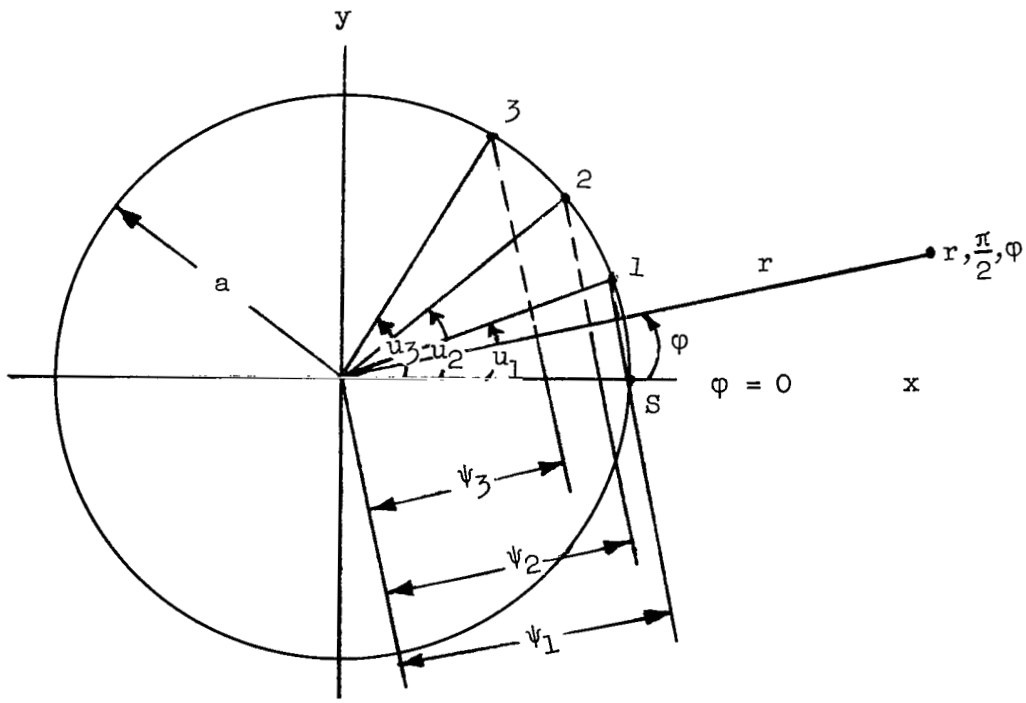

Sketch (c)

Sketch (b) shows a circular array of antennas which are assumed to be identical, equally spaced, and fed in phase. The angular spacing between the antennas is dependent upon the number of antennas under consideration. This dependency is defined as $u_i = \frac{2\pi i}{S}$, where S is the number of antennas with $i = 1, 2, 3, \ldots S$. By restricting an array of radius a to the x,y plane, the position of each antenna can be defined by the coordinates $a, \pi/2, u_i$ with reference to the geometric center of the array.

In sketch (c) the far-field point is assumed to be in the same plane as the array. From the geometry of sketch (c), one can readily see that the distances $\psi_1, \psi_2, \psi_3, \ldots \psi_i$ are:

$$\left.\begin{aligned} \psi_1 &= a_r \cos(u_1 - \varphi) \\ \psi_2 &= a_r \cos(u_2 - \varphi) \\ \psi_3 &= a_r \cos(u_3 - \varphi) \\ &\cdots \\ \psi_i &= a_r \cos(u_i - \varphi) \end{aligned}\right\} \tag{1}$$

where $a_r = \frac{2\pi a}{\lambda} = ka$ is expressed in radians. The principle of superposition is applicable to the determination of the total far-field pattern if the interaction between each element is handled properly. The total far-field pattern for S antennas is written as

$$\Phi = \sum_{i=1}^{S} F(\varphi') e^{j\psi_i} \tag{2}$$

where $F(\varphi')$ represents the single element pattern. Equation (2) may be simplified by assuming the element pattern to be expressible in a Fourier cosine

$$F(\varphi') = \sum_{n=0}^{\infty} a_n \cos^n \varphi'$$

which may be written as

$$F(\varphi') = \sum_{n=0}^{\infty} A_n \cos^n \varphi' \tag{3}$$

where A_n may be complex. As the array in sketch (c) is rotated in the φ direction, the maximum contribution of each antenna to the far-field point occurs when the angle $\varphi - u_i$ vanishes; therefore, the angle φ' may be

replaced by $\varphi - u_i$ in the element function $F(\varphi')$. With this substitution, equation (3) becomes

$$F(\varphi') = \sum_{n=0}^{\infty} A_n \cos^n(\varphi - u_i) \tag{4}$$

From the preceding assumptions and definitions, a step-by-step procedure is given for the derivation of the total far-field pattern. By using equations (1), (2), and (4), the expression representing the total far-field pattern is written as

$$\Phi = \sum_{i=1}^{S} \left[\sum_{n=0}^{\infty} A_n \cos^n(\varphi - u_i) \right] e^{jka \cos(\varphi - u_i)} \tag{5}$$

By letting $Z = ka$ and remembering that A_n is independent of φ', the preceding equation becomes

$$\Phi = \sum_{n=0}^{\infty} A_n (-j)^n \frac{d^n}{dZ^n} \left[\sum_{i=1}^{S} e^{jZ \cos(\varphi - u_i)} \right] \tag{6}$$

From Stratton (ref. 3), the expression

$$e^{jZ \cos(\varphi - u_i)} = \sum_{m=0}^{\infty} (2 - \delta_{om}) j^m J_m(Z) \cos m(\varphi - u_i) \tag{7}$$

enables further reduction. By examining the summation in brackets from equation (6) and using equation (7), the following simplification can be made:

$$\sum_{i=1}^{S} e^{jZ \cos(\varphi - u_i)} = \sum_{m=0}^{\infty} (2 - \delta_{om}) j^m \frac{J_m(Z)}{2} \sum_{i=1}^{S} \left(e^{jm\varphi} e^{\frac{-j2\pi im}{S}} + e^{-jm\varphi} e^{\frac{j2\pi im}{S}} \right)$$

$$\sum_{i=1}^{S} e^{jZ \cos(\varphi - u_i)} = \sum_{m=0}^{\infty} (2 - \delta_{om}) j^m \frac{J_m(Z)}{2} \left(e^{jm\varphi} \sum_{i=1}^{S} e^{\frac{-j2\pi im}{S}} + e^{-jm\varphi} \sum_{i=1}^{S} e^{\frac{j2\pi im}{S}} \right)$$

By letting $q = m/S$, the preceding equation reduces to

$$\sum_{i=1}^{S} e^{jZ \cos(\varphi - u_i)} = S \sum_{q=0}^{\infty} (2 - \delta_{om}) j^m J_m(Z) \cos Sq\varphi \tag{8}$$

when m/S equals an integer. For all noninteger values of m/S, the summations, $\sum_{i=1}^{S} e^{\frac{j2\pi im}{S}}$ and $\sum_{i=1}^{S} e^{\frac{-j2\pi im}{S}}$, equal zero as can be shown by direct expansion. By substituting equation (8) into equation (6), the total far-field pattern for S antennas becomes

$$\Phi = S \sum_{q=0}^{\infty} \left[\sum_{n=0}^{N} A_n (j)^{m-n} \left(\frac{d^n}{dZ^n} J_m(Z) \right) \right] (2 - \delta_{om}) \cos Sq\varphi \qquad (9)$$

When representing any curve by a Fourier series, a finite number of terms is obviously taken; therefore, the upper limit on the Fourier summation has been replaced by N. By examining the series representation of the Bessel function, $\sum_{q=0}^{\infty} J_m(Z)$, it is obvious that within a few terms the series converges provided the order of the Bessel function exceeds its argument for a large number of antennas. By using this convergence property and assuming that the number of terms in the Fourier series is less than the number of antennas, equation (9) becomes

$$\Phi \approx S \sum_{n=0}^{N} A_n (-j)^n \frac{d^n}{dZ^n} \left(J_o(Z) + 2j^S J_S(Z) \cos S\varphi \right) \qquad (N < S) \quad (10)$$

where δ_{om} is one for $q = 0$ and zero for $q \geq 1$. Equation (10) is an approximation for the total far-field pattern when the circumference in wavelengths Z is less than the number of sources S.

COMPUTATIONS

By using equation (10), the graphs appearing in figures 1 to 3 were plotted. To see clearly how equation (10) is used, the far-field equations for each element pattern, $F(\varphi') = 1$, $F(\varphi') = 1 + \cos \varphi'$, and $F(\varphi') = 1 + \frac{1}{2} \cos \varphi'$ are written explicitly. To visualize the element (antenna) patterns, see sketch (a). The total far-field pattern equations for these element patterns are written as follows:

For $F(\varphi') = 1$:

$$\Phi = S \left(J_o(Z) + 2j^S J_S(Z) \cos S\varphi \right) \qquad (11)$$

For $F(\varphi') = 1 + \cos \varphi'$:

$$\Phi = S\left[\left(J_o(Z) + 2j^S J_S(Z)\cos S\varphi\right) - j\left(J_o'(Z) + 2j^S J_S'(Z)\cos S\varphi\right)\right] \tag{12}$$

For $F(\varphi') = 1 + \frac{1}{2}\cos \varphi'$:

$$\Phi = S\left[\left(J_o(Z) + 2j^S J_S(Z)\cos S\varphi\right) - \frac{j}{2}\left(J_o'(Z) + 2j^S J_S'(Z)\cos S\varphi\right)\right] \tag{13}$$

where the primes on the Bessel functions denote the first derivative with respect to Z.

Data for the magnitudes of equations (11), (12), and (13) were calculated by machine for the following ranges and incremental changes:

$$\left.\begin{array}{ll} 1 \leqq Z \leqq 60 & \Delta Z = 0.2 \\ Z \leqq S \leqq 3/2Z & \Delta S = 1.0 \\ 0 \leqq \varphi \leqq 2\pi/S & \Delta\varphi = 0.5 \end{array}\right\} \tag{14}$$

In addition to these restrictions, the number of antennas must remain an integer. For each of the three equations, the magnitudes were calculated as φ varied from zero to $2\pi/S$ for a particular Z and S.

By examining the data for each Z and S as φ varied, the ratios of maximum to minimum magnitudes were computed manually. The amount of ripple or fluctuation in the far-field pattern is defined in decibels as $20 \log_{10} \frac{|\Phi|_{max}}{|\Phi|_{min}}$, where $\frac{|\Phi|_{max}}{|\Phi|_{min}}$ is the ratio of maximum magnitude to minimum magnitude. These fluctuations were plotted in figures 1 to 3 as a function of Z for each S. Good agreement (within a few tenths of a decibel) was obtained when these curves were compared with the curves given by Chu. Table I gives the Z and S ranges of the elements used in the computations.

CONCLUDING REMARKS

In the omnidirectional case, the fluctuations decrease as the number of antennas increases, except at the discontinuities. At these discontinuities the fluctuations approach infinity independently of the number of antennas.

These undesirable points occur at values of circumference in wavelengths which cause the Bessel function $J_0(Z)$ to approach zero.

In the other two cases, no discontinuities exist since the minimum magnitude is never $|J_0(Z)|$. However, the fluctuations decrease as the number of antennas increases but not in the same manner as in the omnidirectional case.

The reason for the decrease in fluctuation as a result of the increasing number of antennas for both omnidirectional and nonomnidirectional element patterns is that the spacing between the elements obviously decreases, and thus causes the ripple in the far-field pattern to be smaller. If the spacing between elements were made extremely small, the far-field pattern would approach a circle.

In using the derived equation, one must stay within the approximation stated; that is, the circumference in wavelengths must be less than the number of sources. This requirement means that the spacing between the sources is less than a wavelength.

Langley Research Center,
National Aeronautics and Space Administration,
Langley Station, Hampton, Va., August 5, 1964.

REFERENCES

1. Kraus, John D.: Antennas. McGraw-Hill Book Co., Inc., 1950.

2. Chu, Ta-Shing: On the Use of Uniform Circular Arrays to Obtain Omnidirectional Patterns. IRE Trans. on Antennas and Propagation, vol. AP-7, no. 4, Oct. 1959, pp. 436-438.

3. Stratton, Julius Adams: Electromagnetic Theory. McGraw-Hill Book Co., Inc., 1941.

TABLE I.- RANGES FOR ELEMENTS

Range of -		Figure
S	Z	
$F(\varphi') = 1$		
3 to 14	1 to 10	1(a)
14 to 26	10 to 20	1(b)
21 to 40	20 to 30	1(c)
31 to 49	30 to 40	1(d)
43 to 60	40 to 50	1(e)
53 to 70	50 to 60	1(f)
$F(\varphi') = 1 + \cos \varphi'$		
4 to 14	1 to 10	2(a)
11 to 28	10 to 20	2(b)
21 to 39	20 to 30	2(c)
32 to 48	30 to 40	2(d)
43 to 60	40 to 50	2(e)
53 to 68	50 to 60	2(f)
$F(\varphi') = 1 + \frac{1}{2} \cos \varphi'$		
4 to 14	1 to 10	3(a)
12 to 28	10 to 20	3(b)
21 to 38	20 to 30	3(c)
32 to 49	30 to 40	3(d)
43 to 60	40 to 50	3(e)
53 to 70	50 to 60	3(f)

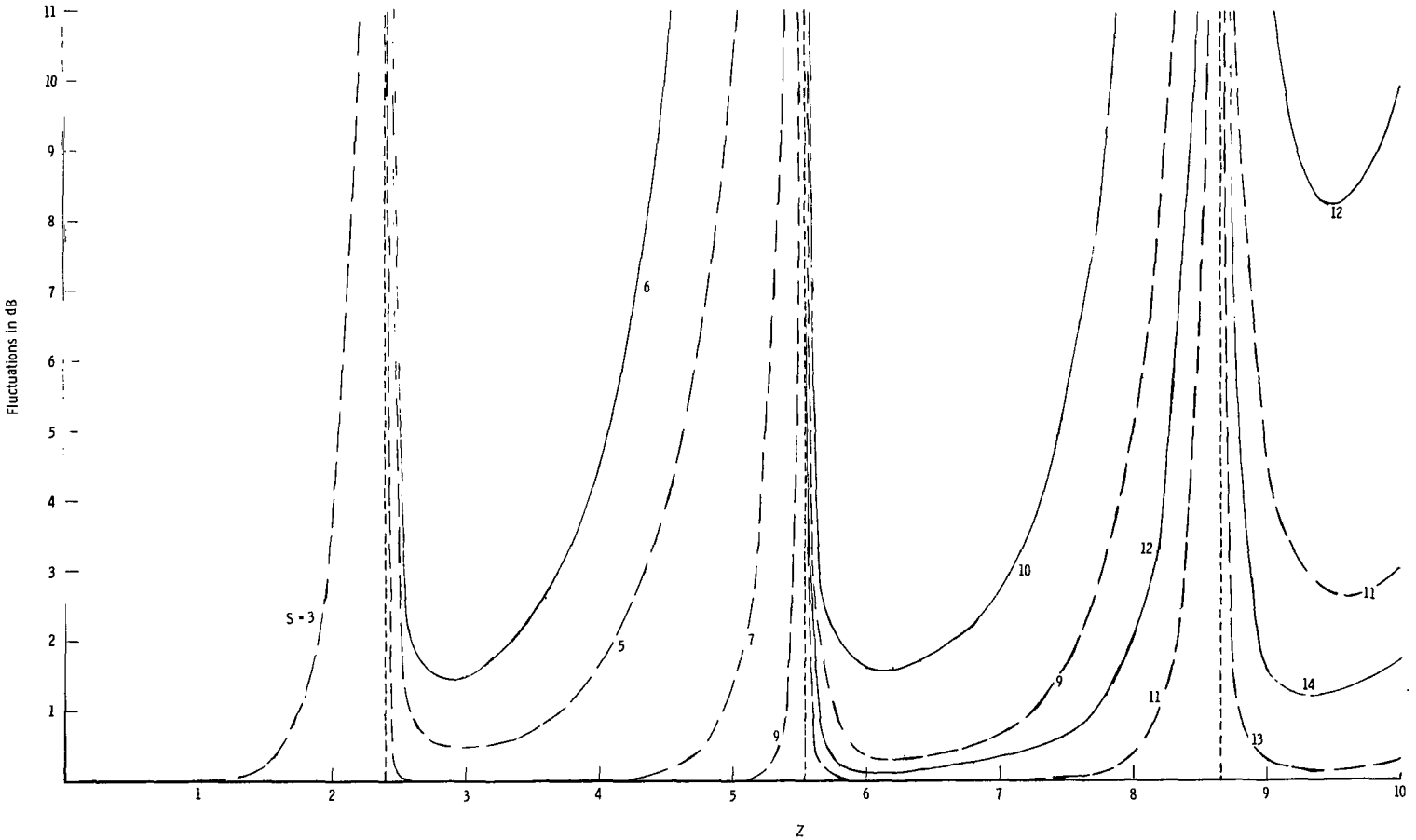

(a) Z = 1 to 10.

Figure 1.- The azimuthal fluctuations of a uniform circular array having the element pattern $F(\varphi') = 1$. Z = ka. As S increases, the curves asymptotically approach the zero dB level except at the discontinuities. As S decreases, the fluctuations become extremely large.

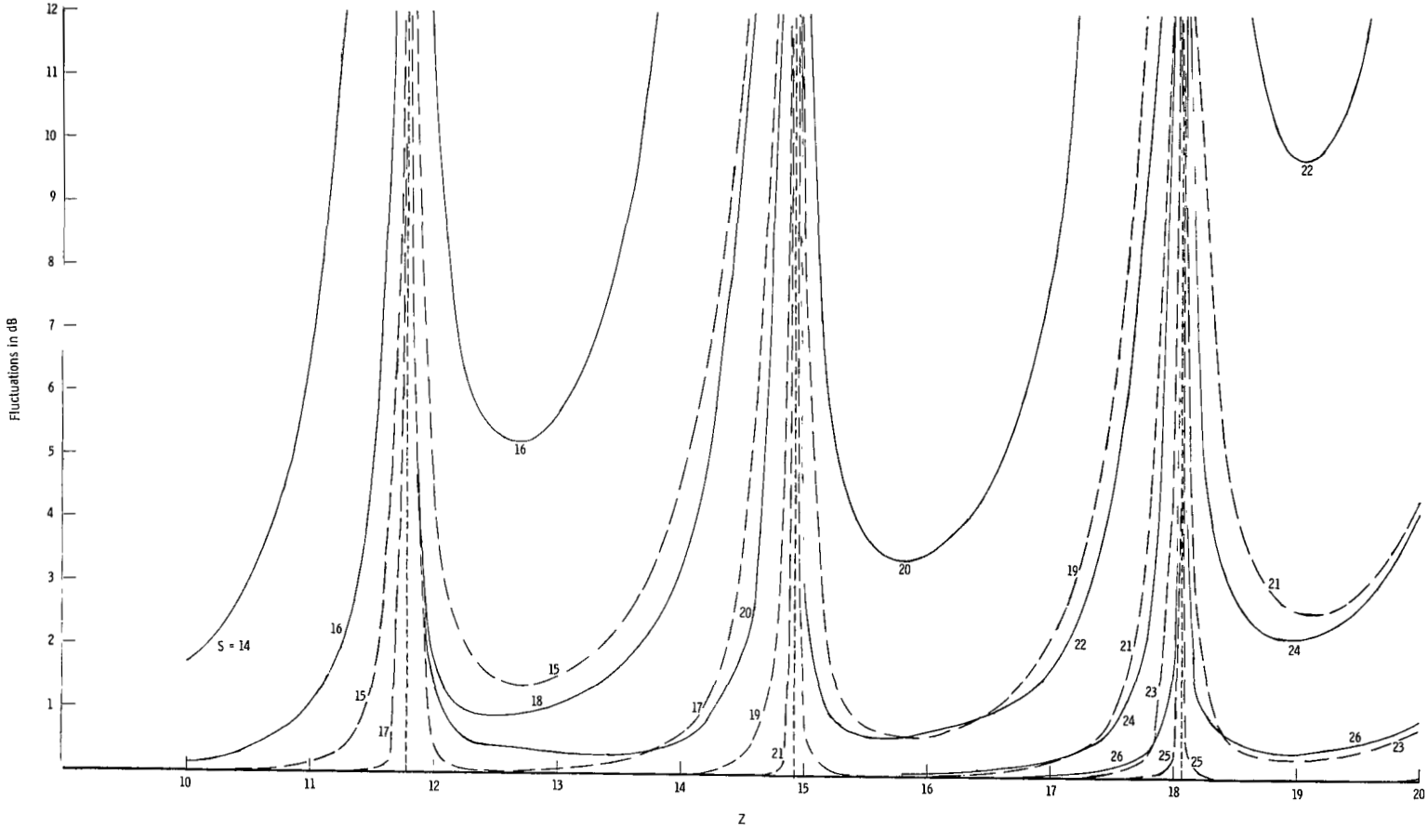

(b) Z = 10 to 20.

Figure 1.- Continued.

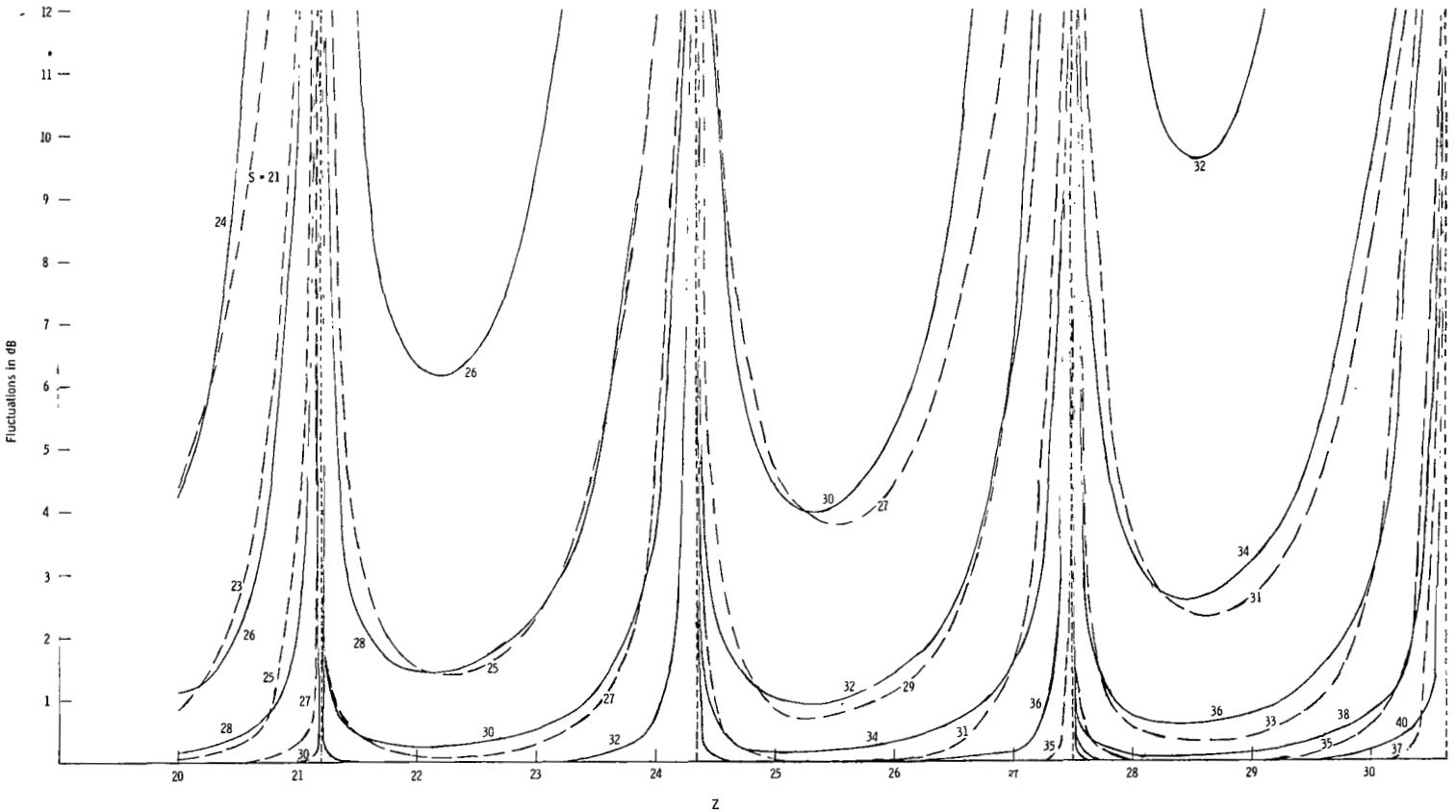

(c) Z = 20 to 30.

Figure 1.- Continued.

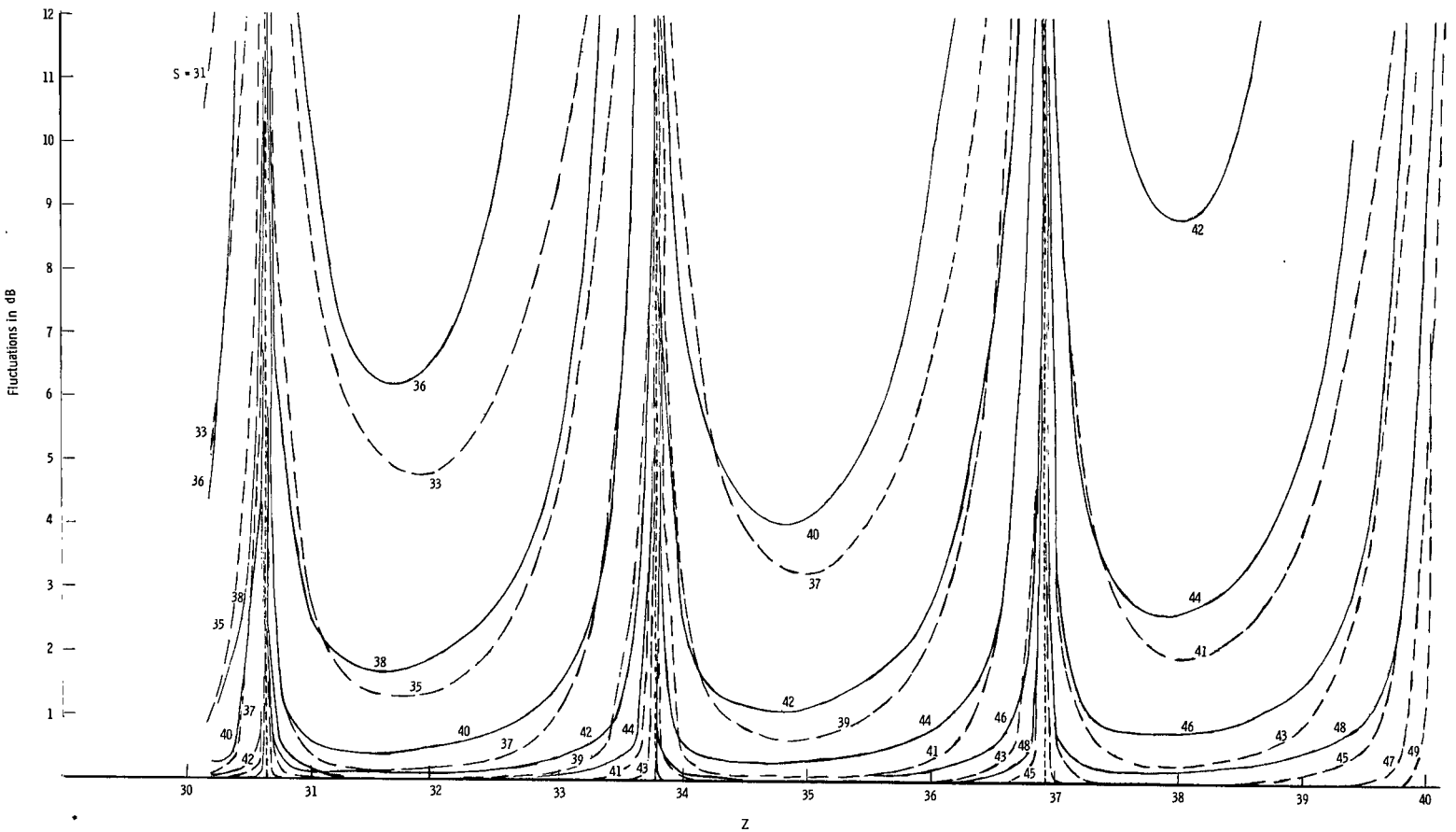

(d) Z = 30 to 40.

Figure 1.- Continued.

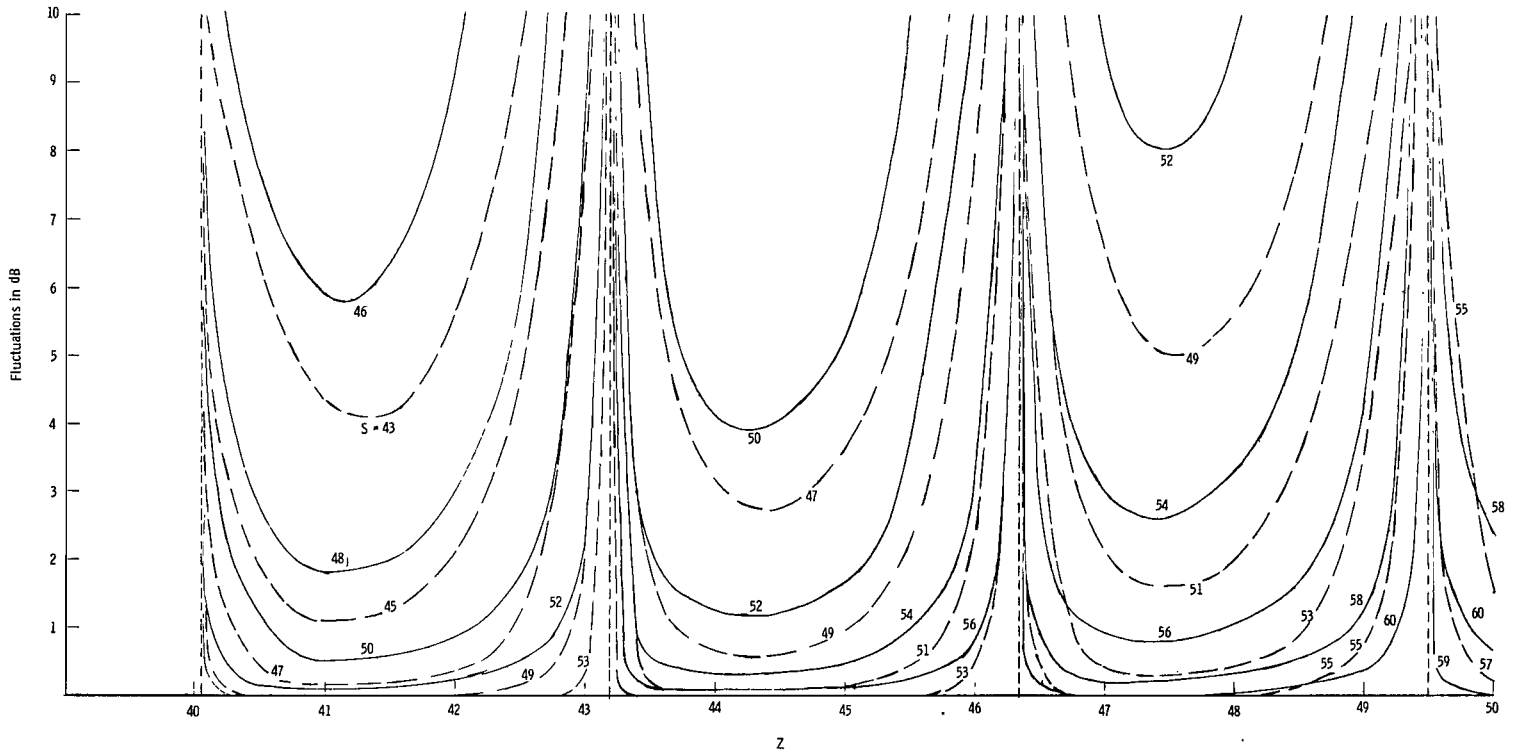

(e) Z = 40 to 50.

Figure 1.- Continued.

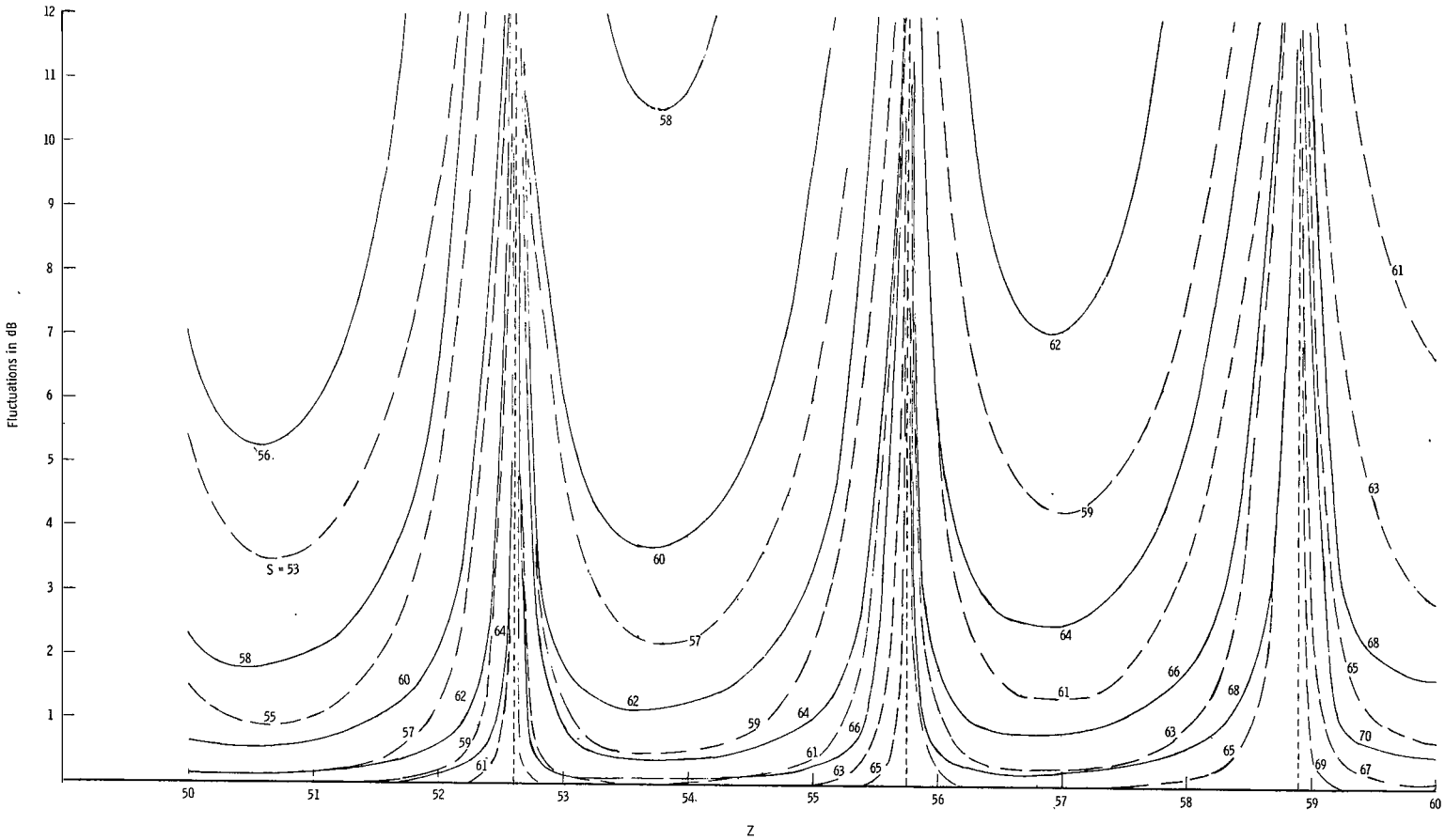

(f) Z = 50 to 60.

Figure 1.- Concluded.

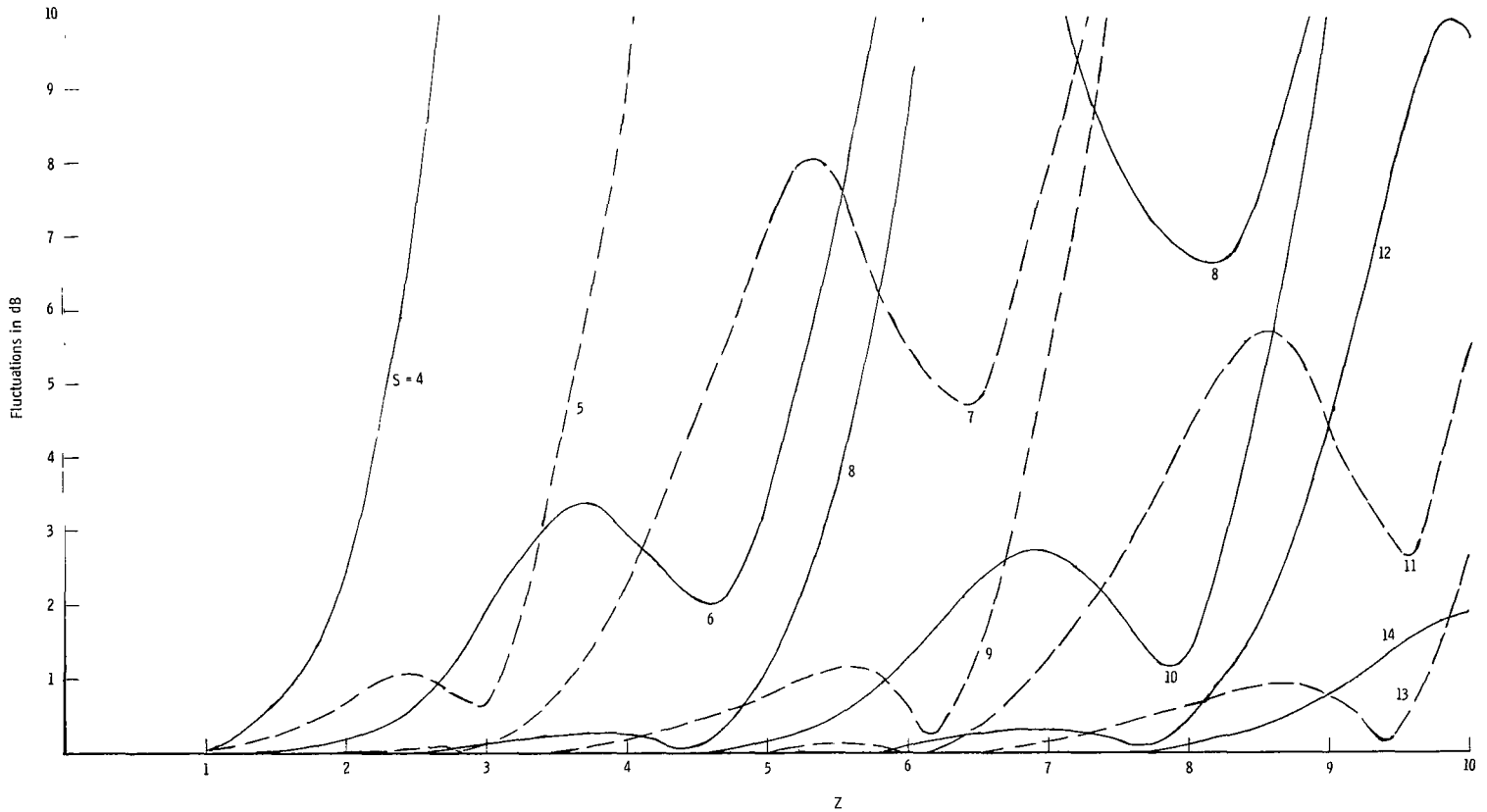

(a) Z = 1 to 10.

Figure 2.- The azimuthal fluctuations of a uniform circular array having the element pattern $F(\varphi') = 1 + \cos \varphi'$. Z = ka. The fluctuations become extremely small as S increases and large as S decreases.

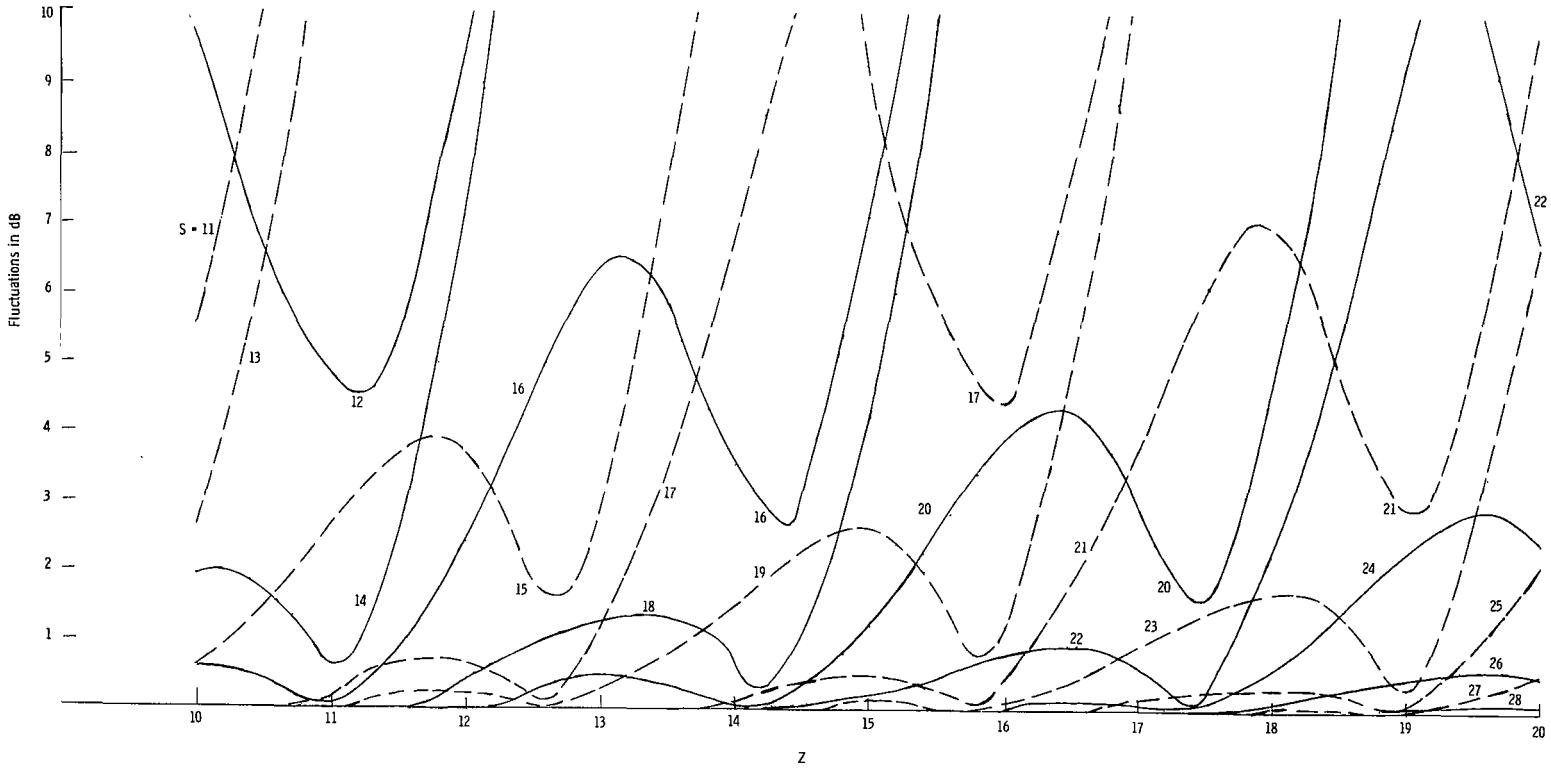

(b) Z = 10 to 20.

Figure 2.- Continued.

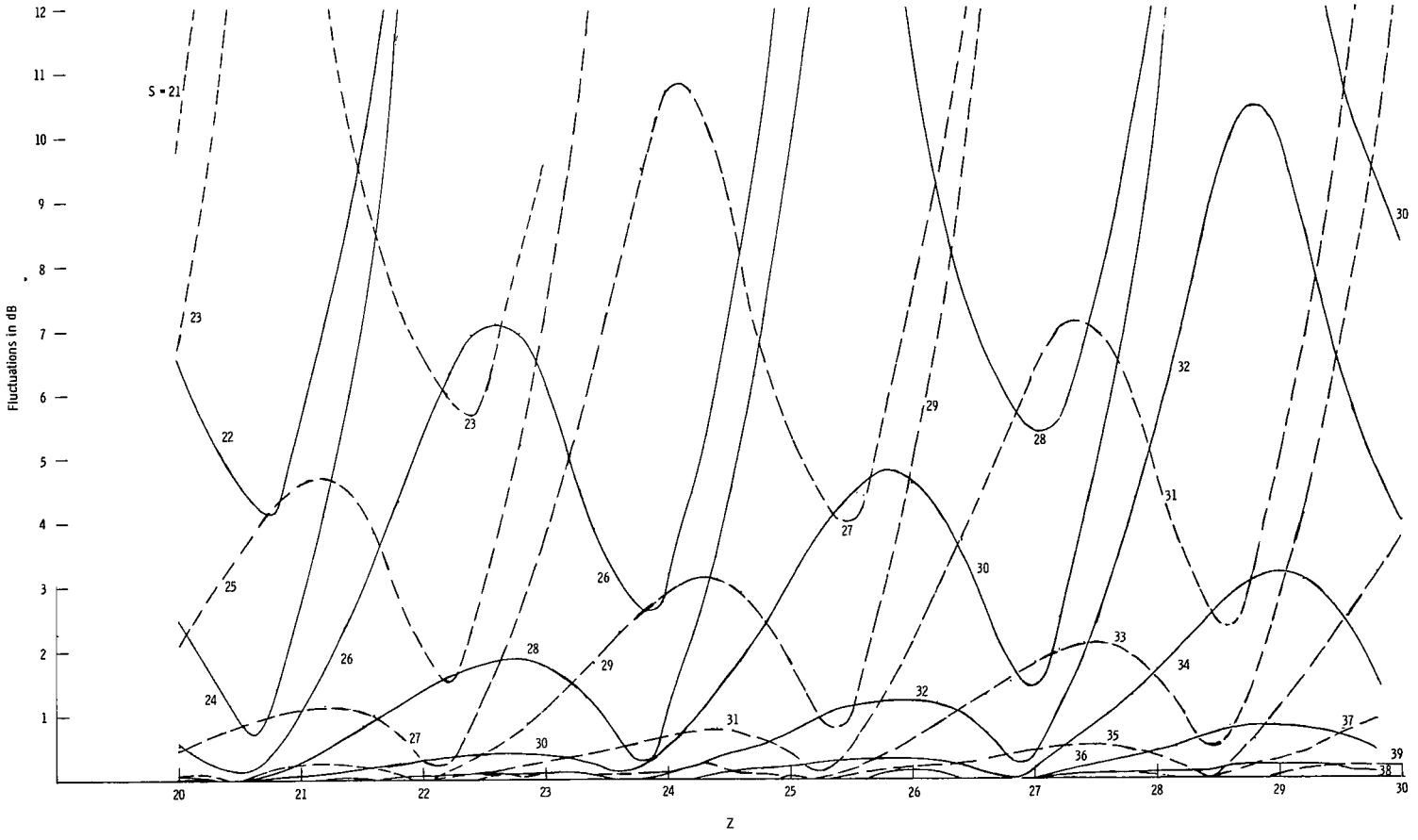

(c) Z = 20 to 30.

Figure 2.- Continued.

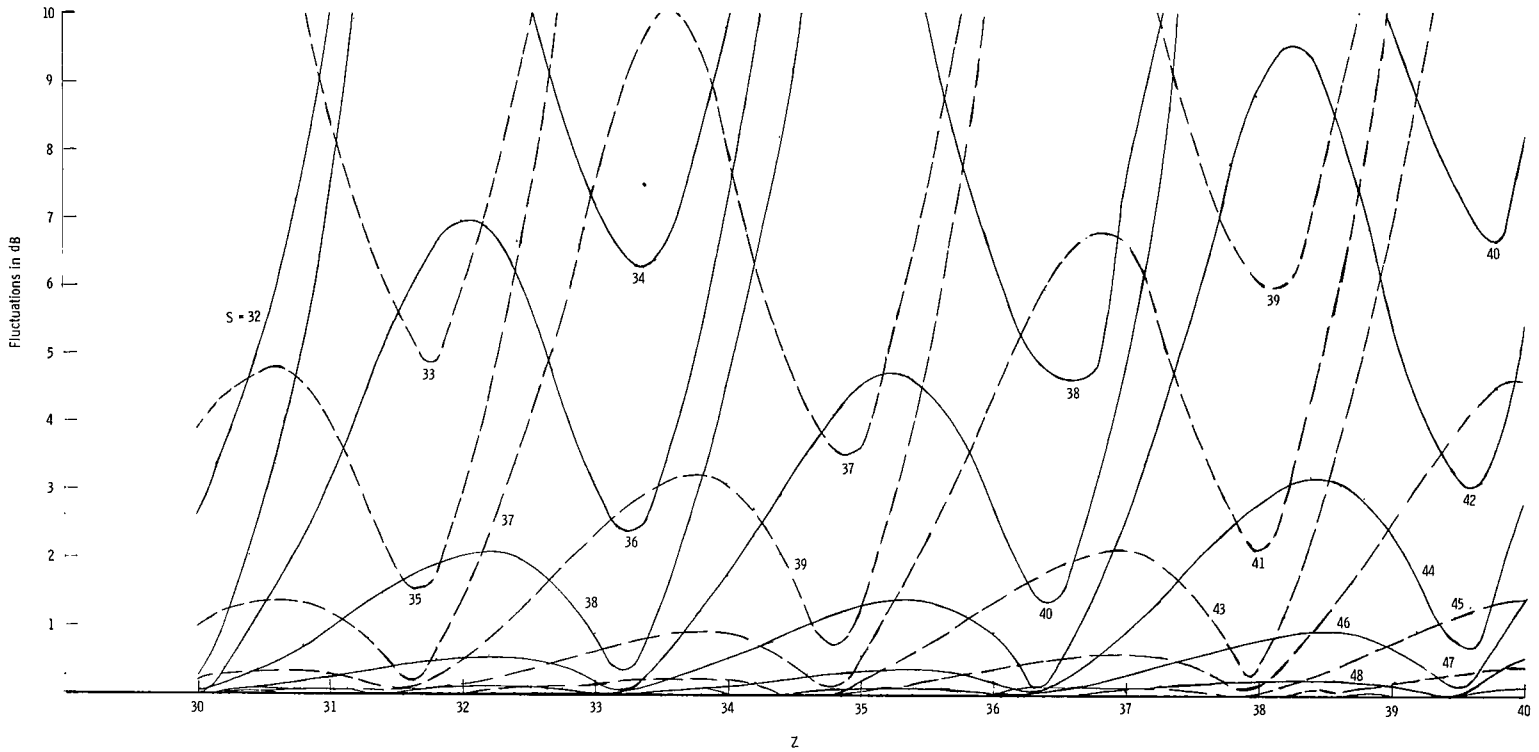

(d) Z = 30 to 40.

Figure 2.- Continued.

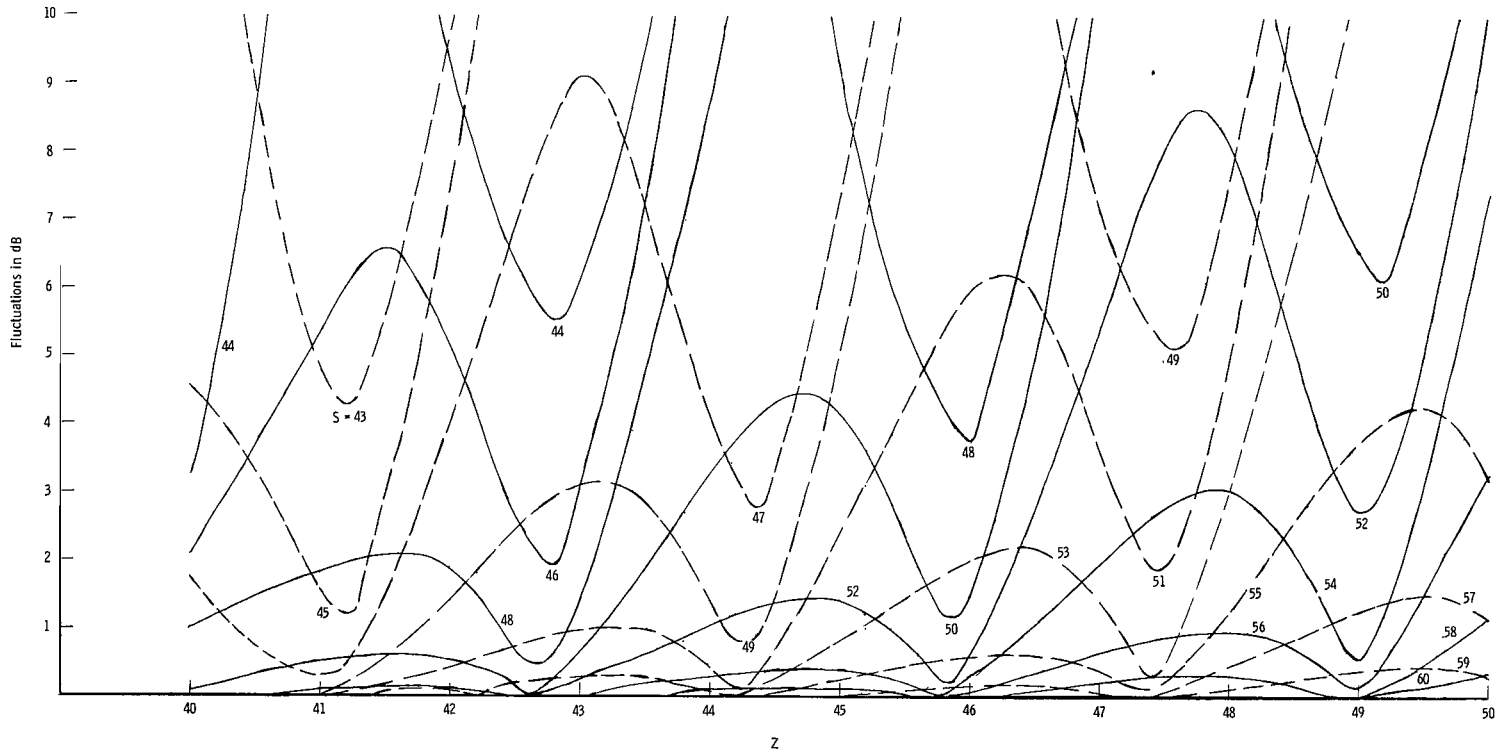

(e) Z = 40 to 50.

Figure 2.- Continued.

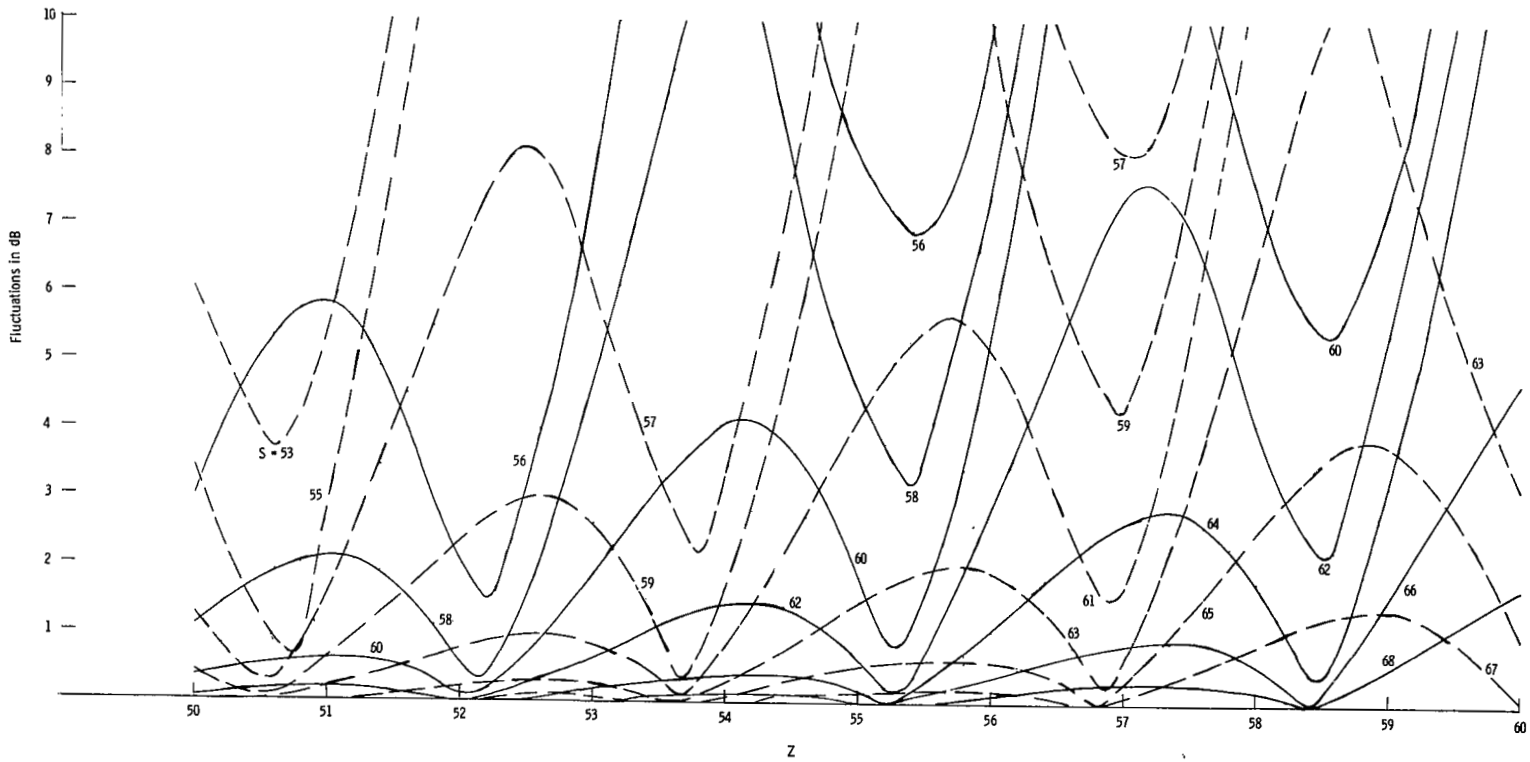

(f) Z = 50 to 60.

Figure 2.- Concluded.

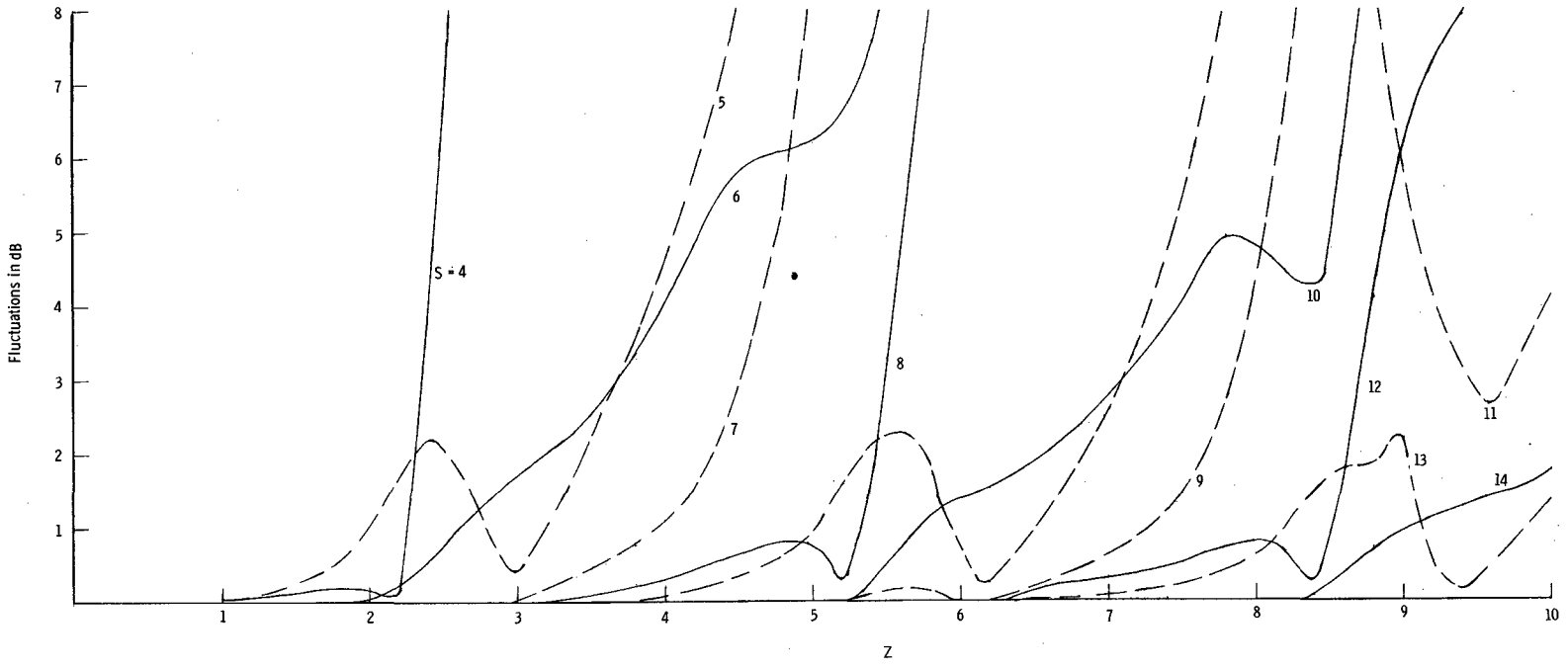

(a) Z = 1 to 10.

Figure 3.- The azimuthal fluctuations of a uniform circular array having the element pattern $F(\varphi') = 1 + \frac{1}{2}\cos\varphi'$. Z = ka. The fluctuations become extremely small as S increases and large as S decreases.

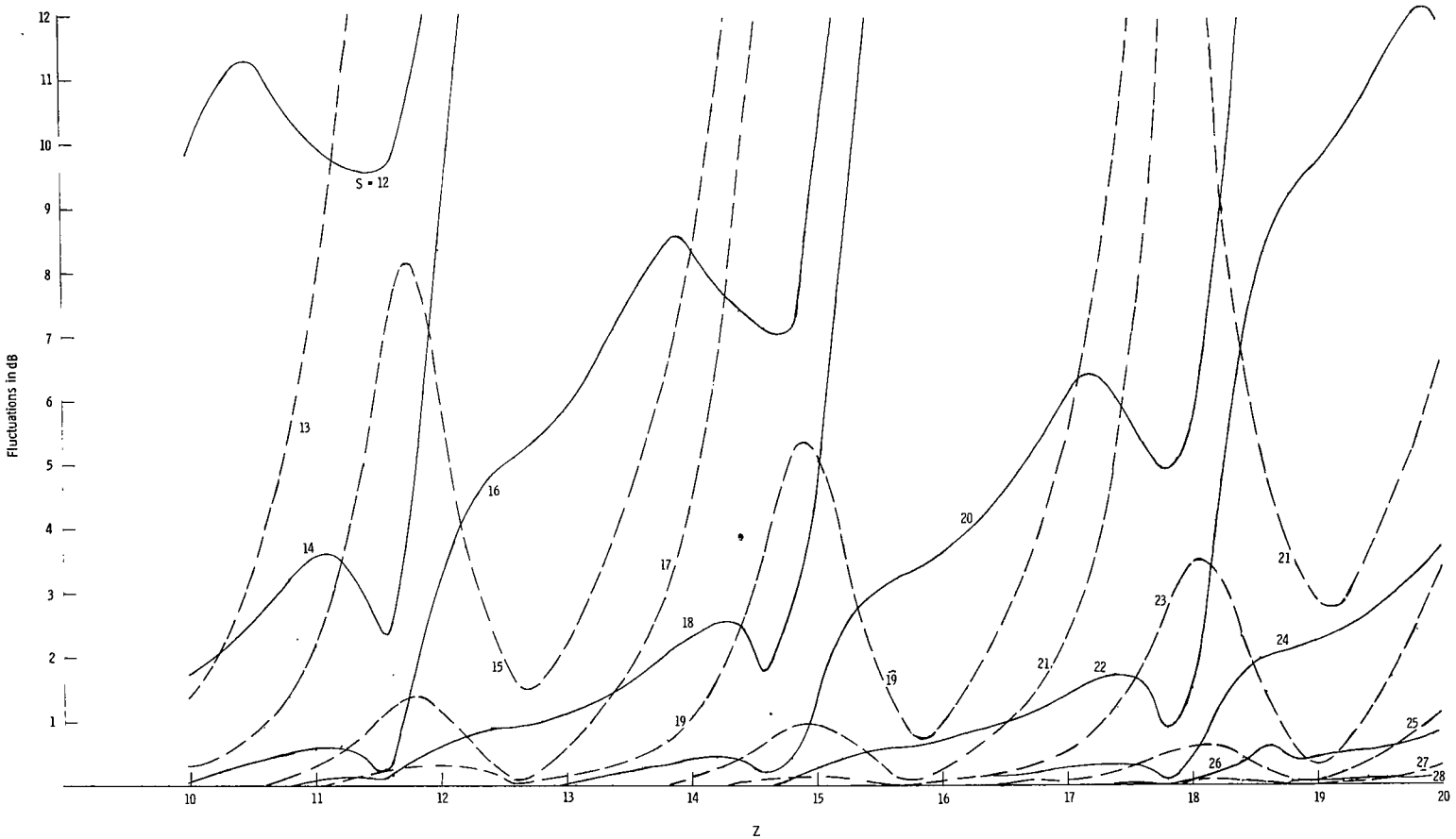

(b) Z = 10 to 20.

Figure 3.- Continued.

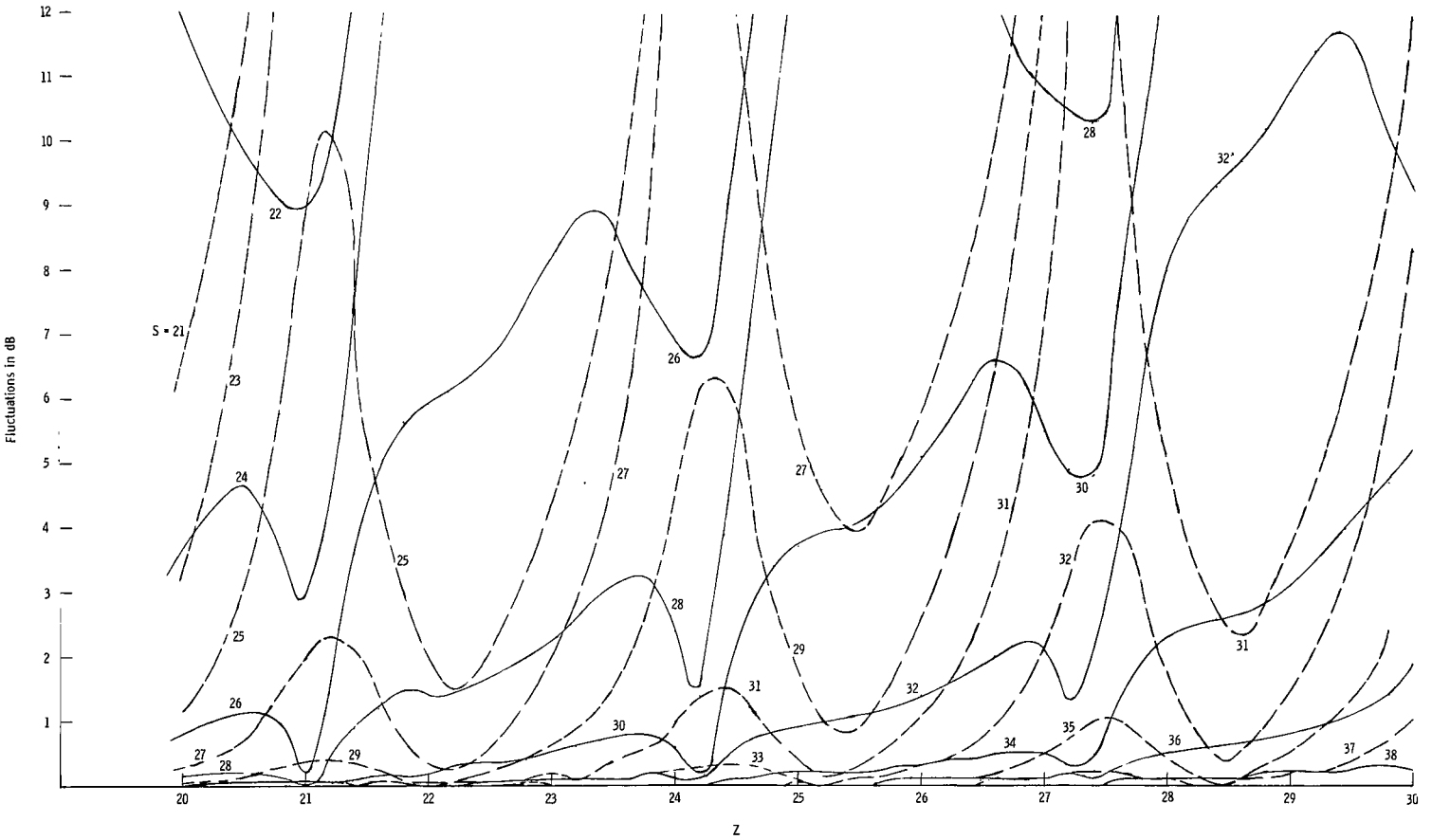

(c) Z = 20 to 30.

Figure 3.- Continued.

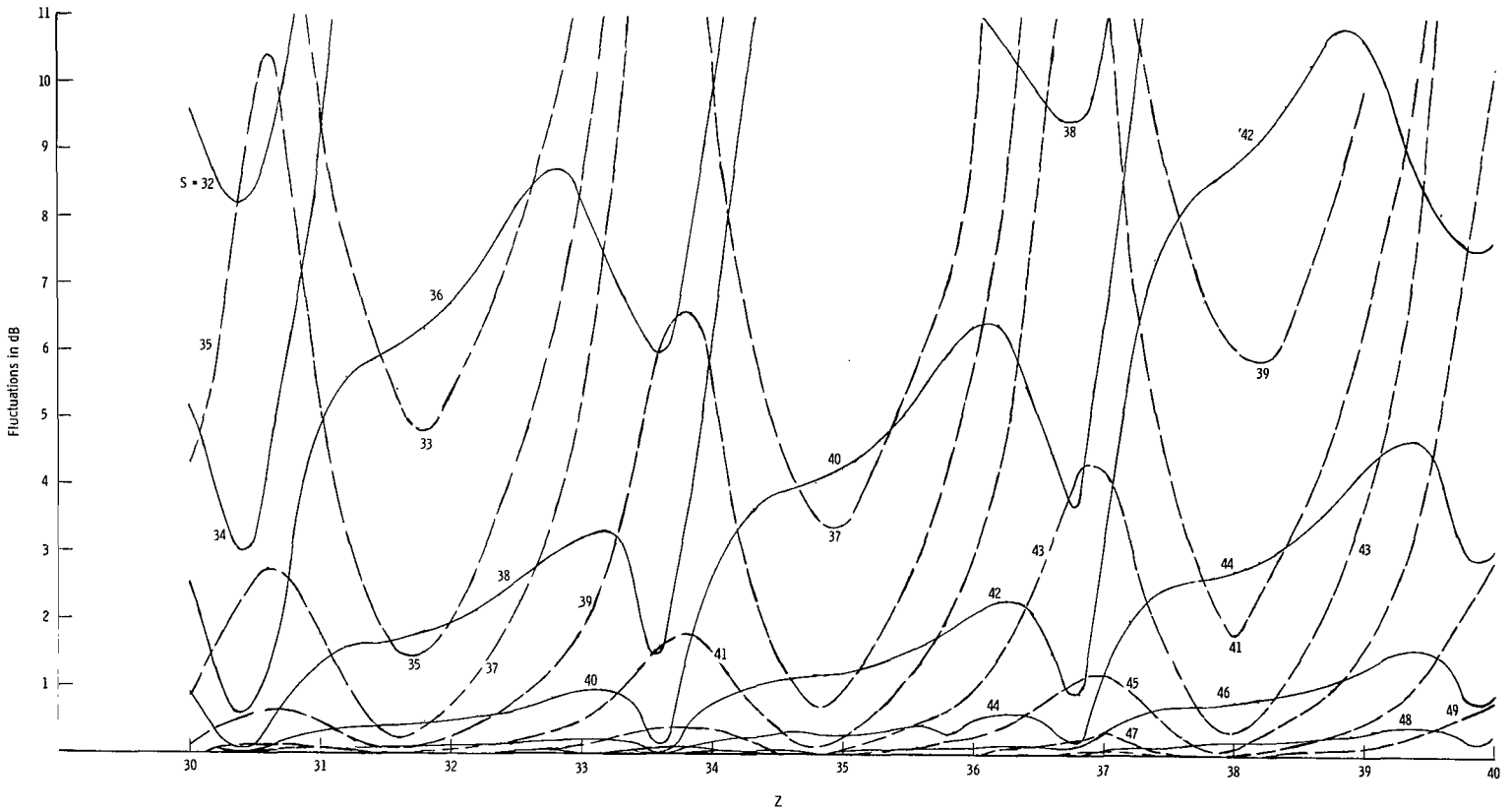

(d) Z = 30 to 40.

Figure 3.- Continued.

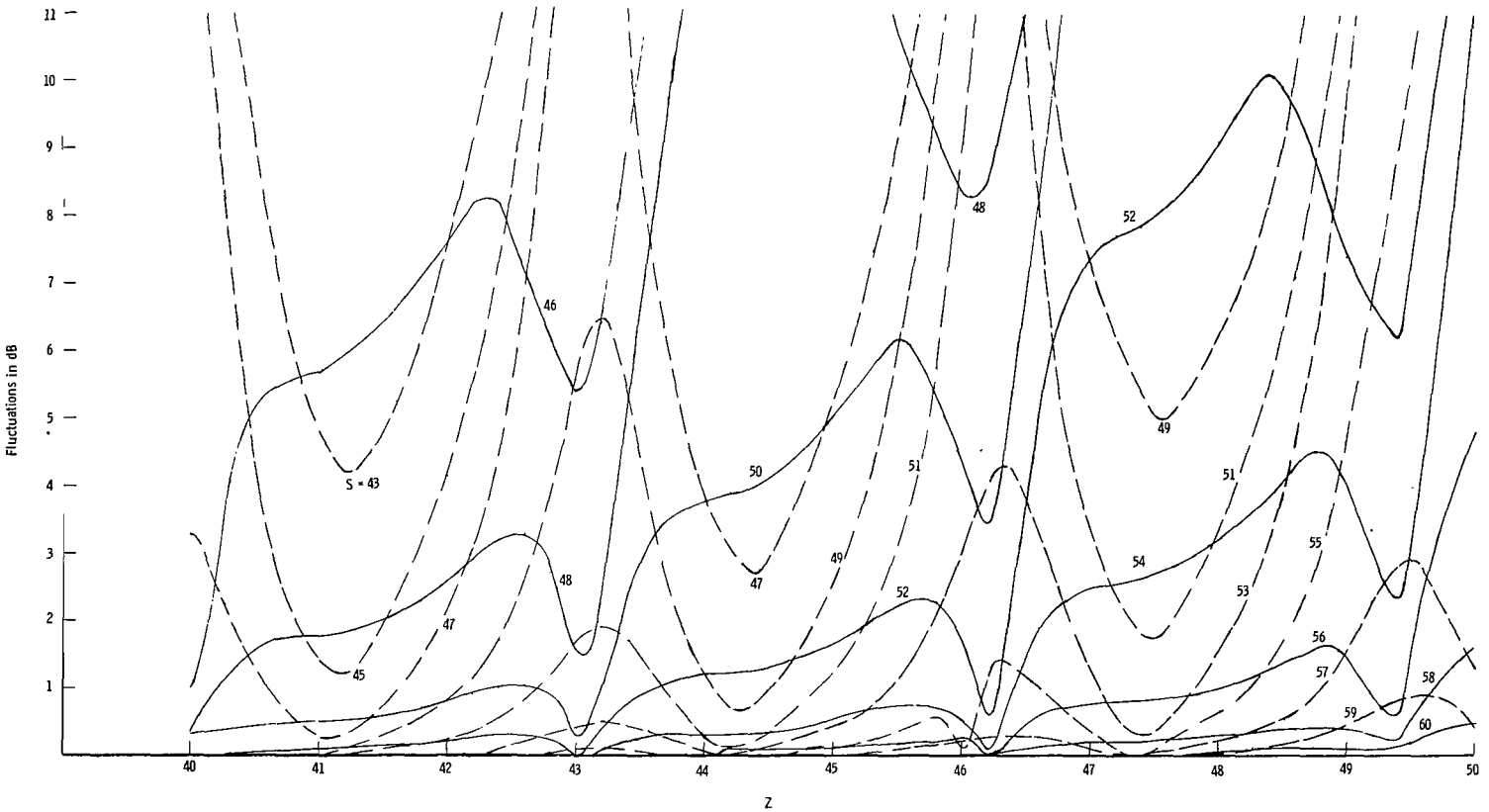

(e) Z = 40 to 50.

Figure 3.- Continued.

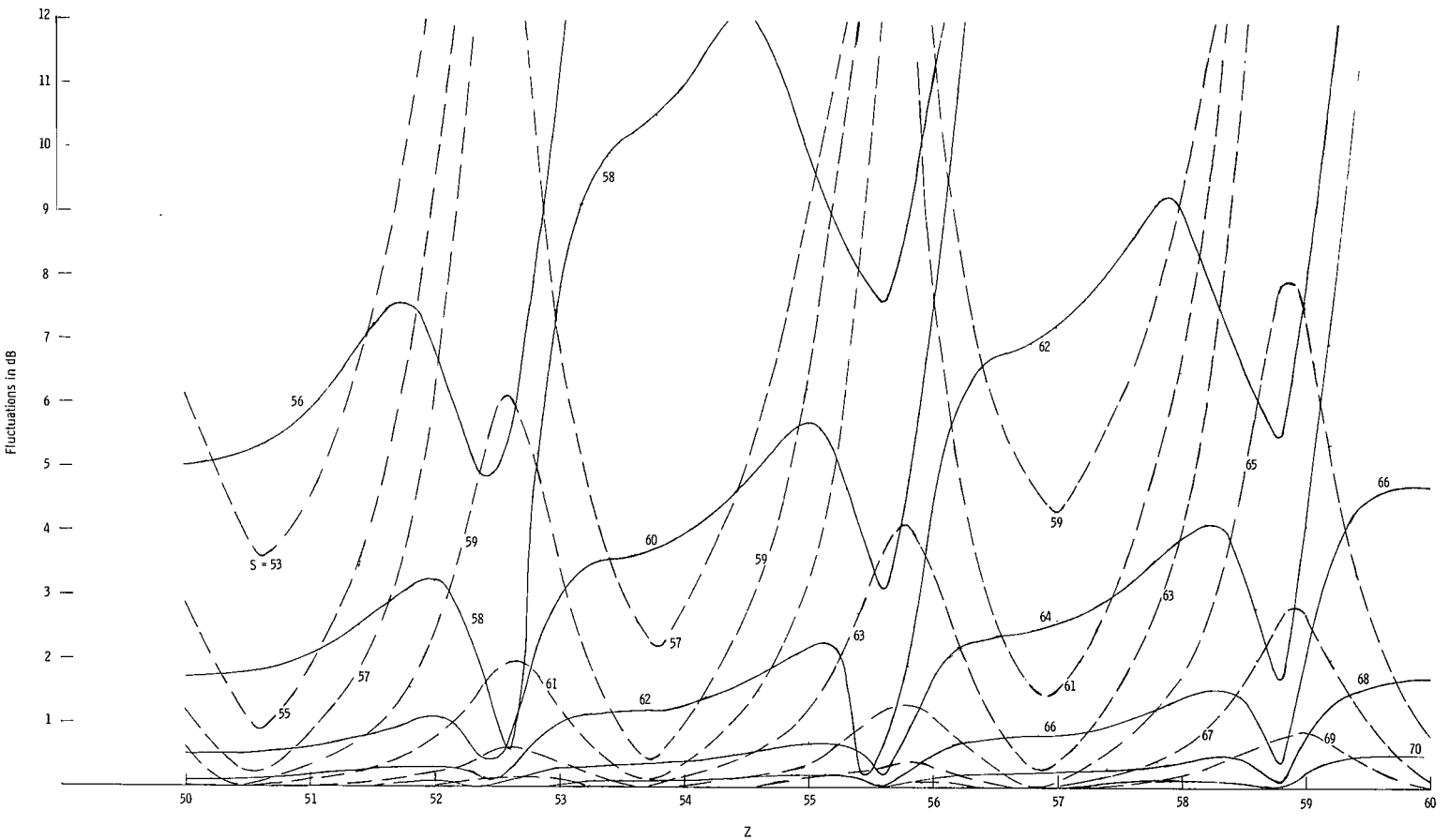

(f) Z = 50 to 60.

Figure 3.- Concluded.

"The aeronautical and space activities of the United States shall be conducted so as to contribute . . . to the expansion of human knowledge of phenomena in the atmosphere and space. The Administration shall provide for the widest practicable and appropriate dissemination of information concerning its activities and the results thereof."

—NATIONAL AERONAUTICS AND SPACE ACT OF 1958

NASA SCIENTIFIC AND TECHNICAL PUBLICATIONS

TECHNICAL REPORTS: Scientific and technical information considered important, complete, and a lasting contribution to existing knowledge.

TECHNICAL NOTES: Information less broad in scope but nevertheless of importance as a contribution to existing knowledge.

TECHNICAL MEMORANDUMS: Information receiving limited distribution because of preliminary data, security classification, or other reasons.

CONTRACTOR REPORTS: Technical information generated in connection with a NASA contract or grant and released under NASA auspices.

TECHNICAL TRANSLATIONS: Information published in a foreign language considered to merit NASA distribution in English.

TECHNICAL REPRINTS: Information derived from NASA activities and initially published in the form of journal articles.

SPECIAL PUBLICATIONS: Information derived from or of value to NASA activities but not necessarily reporting the results of individual NASA-programmed scientific efforts. Publications include conference proceedings, monographs, data compilations, handbooks, sourcebooks, and special bibliographies.

Details on the availability of these publications may be obtained from:

SCIENTIFIC AND TECHNICAL INFORMATION DIVISION

NATIONAL AERONAUTICS AND SPACE ADMINISTRATION

Washington, D.C. 20546